Degradation and Performance Issues of MIMO/OFDM in the Presence of Motion

Pedro Tejera, Mario Castaneda, Faruck Morcos, Wolfgang Utschick
Institute for Circuit Theory and Signal Processing
Arcisstrasse 21, Munich University of Technology, 80290 Munich, Germany
Email: {tejera,utschick}@nws.ei.tum.de
Phone: +49-89-289-28514, Fax: +49-89-289-28504

Abstract— **Different degrees of channel knowledge at the transmitter lead to different transmission strategies with disparate performance in a multiple-input multiple-output (MIMO), orthogonal frequency-division multiplexing (OFDM) system. While in a frequency-division duplex (FDD) scheme instantaneous channel knowledge requires the feedback of channel state information (CSI) from the receiver, which depending on system parameters might be prohibitive, in a time-division duplex (TDD) system, channel estimates obtained during reception can be made use of during transmission. Thereby, the basic problem is obsolescence of CSI over a frame interval. In the work at hand, applying transmission strategies that adapt to the channel as much as the available CSI allows, performance of a TDD MIMO/OFDM system is compared and discussed for four degrees of CSI: The theoretical case of perfect instantaneous CSI, perfect CSI that becomes outdated during the transmission of a frame, partial CSI, where partial refers to the knowledge of the transmit correlation matrix of the channel, and finally, the case of no CSI. To this end, a channel model is introduced that permits the simulation of channel variations due to mobility for different spatial and temporal spreads.**

I. Introduction

The combination of OFDM and MIMO seems to be very promising when aiming at the design of very high-rate wireless mobile systems [1]. While multiple antennas at the transmitter and receiver elevate channel capacity, i.e. the achievable transmission rate, OFDM converts the wideband frequency-selective radio channel into a set of parallel flat-fading channels, thus simplifying signal processing required at the receiver [2].

Most of the work done so far assumes perfect CSI at the receiver, which is a realistic assumption. However, looking at the transmitter, assumptions range from perfect instantaneous CSI, e.g. [2] [3] [4], to no CSI at all, e.g. [5] [6] [7], which results in very different transmission approaches. Applying a V-BLAST-like detector at the receiver [8], this paper evaluates and compares the performance of the downlink of a TDD MIMO/OFDM system for four different degrees of channel knowledge: perfect instantaneous CSI, perfect CSI with obsolescence, partial CSI and no CSI. While the first is highly idealistic and is only included as a theoretical bound, the last might be deemed overconservative. Specially interesting will be the comparison between the remaining two cases. On the one hand partial CSI is easier to obtain than perfect CSI and as long as the channel remains stationary mobility should not affect performance. On the other hand perfect CSI permits the application of bit and power loading over frequency, which is expected to yield a good performance though it is bound to degrade due to mobility.

This comparison primarily serves two purposes. Observing performance degradation over time we can better judge the usefulness of channel prediction or other methods that take into account CSI obsolescence. On the other hand, taking into account the different complexity of each of the approaches, we will be able to get a feeling about the most convenient transmission scheme for a certain kind of scenario.

In order to compare performance in different scenarios a flexible channel model has been developed that captures the stochastic nature of radio channels and at the same time permits the simulation of channel variation due to mobility. The main peculiarity of this model is that different from other existing models of frequency-selective MIMO channels, e.g. [5] [9], no assumptions are made about the statistics of the channel and no random nature of single propagation paths must be postulated, which proves difficult to justify, cf. [10]. Instead, in our model randomness is the natural consequence of a random characterization of the location of the mobile unit.

The remaining of the paper is structured as follows. Section II describes the parametric channel model which has been used in this work. In Section III simulation settings are listed and discussed. Section IV presents simulation results and finally, in Section V conclusions are drawn.

II. Channel Model

Three coordinate systems form the basis of this model (s. Fig. 1). $\mathcal{O}_{\mathrm{Tx}}$ is placed on one of the array elements at the base station, $\mathcal{O}_{\mathrm{E}}$ is associated with a stationarity region E, within which the mobile unit is supposed to be located. These two coordinate systems are assumed to be static. Finally, $\mathcal{O}_{\mathrm{Rx}}$ is placed on one of the array elements at the mobile unit and is mobile with respect to the two coordinate systems defined previously.

In the model, each path $\ell \in \{1,\ldots,L\}$ is parameterized by a delay τ_ℓ, a complex-valued attenuation α_ℓ, a direction of departure $\vec{\Omega}_\ell^{\mathrm{Tx}}$ and a direction of arrival $\vec{\Omega}_\ell^{\mathrm{Rx}}$. Parameters τ_ℓ and α_ℓ are defined with respect to $\mathcal{O}_{\mathrm{E}}$ and the stationarity region E is defined as the spatial area around $\mathcal{O}_{\mathrm{E}}$ within which, due to a far-field assumption $R \gg r$, parameters $|\alpha_\ell|$, τ_ℓ, $\vec{\Omega}_\ell^{\mathrm{Tx}}$

0-7803-8255-2/04/$20.00 ©2004 IEEE.

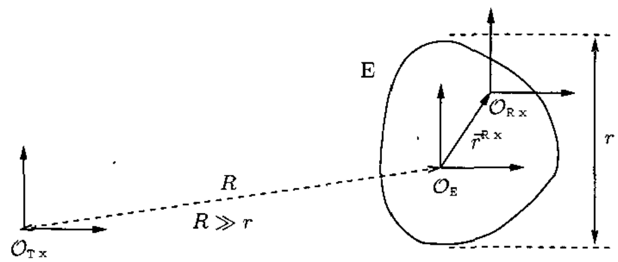

Fig. 1. Coordinate systems

and $\vec{\Omega}_\ell^{\mathrm{Rx}}$ can be taken as constant. α_ℓ's are assumed to be time and frequency invariant. The first assumption means that scatterers are static and therefore time variation is exclusively caused by a change of position of the mobile unit. The second assumption means that different propagation delays will be the only source of frequency selectivity.

Given the parametric model described above, for a particular frequency f the transfer function between transmit antenna $n \in \{1, \dots, M_t\}$ with position vector $\vec{r}_n^{\,\mathrm{Tx}}$ with respect to $\mathcal{O}_{\mathrm{Tx}}$ and receive antenna $m \in \{1, \dots, M_r\}$ with position vector $\vec{r}_m^{\,\mathrm{Rx}}$ with respect to $\mathcal{O}_{\mathrm{Rx}}$ is given by

$$H(\vec{r}_n^{\,\mathrm{Tx}}, \vec{r}_m^{\,\mathrm{Rx}}, \vec{r}^{\,\mathrm{Rx}}, f) = \sum_{\ell=1}^{L} \underbrace{e^{-j\frac{2\pi}{\lambda}\vec{r}_m^{\,\mathrm{Rx}}\vec{\Omega}_l^{\mathrm{Rx}}}}_{(a_{m,\ell}^{\mathrm{Rx}})^*} \underbrace{\alpha_\ell e^{-j\frac{2\pi}{\lambda}\vec{r}^{\,\mathrm{Rx}}\vec{\Omega}_\ell^{\mathrm{Rx}}} e^{-j2\pi f \tau_\ell}}_{d_\ell} \underbrace{e^{j\frac{2\pi}{\lambda}\vec{r}_n^{\,\mathrm{Tx}}\vec{\Omega}_\ell^{\mathrm{Tx}}}}_{a_{n,\ell}^{\mathrm{Tx}}}. \quad (1)$$

Thereby, λ is the wavelength corresponding to frequency f and $\vec{r}^{\,\mathrm{Rx}}$ indicates the position of the mobile unit with respect to $\mathcal{O}_{\mathrm{E}}$. Each term in Eq. 1 consists of three factors: $a_{n,\ell}^{\mathrm{Tx}}$ and $a_{m,\ell}^{\mathrm{Rx}}$, which depend on the array geometry at the base station and mobile unit respectively, and d_ℓ, which only depends on the propagation environment and the location of the mobile unit. Considering all array elements at the transmitter and receiver the resulting MIMO channel matrix can be expressed in compact form as

$$\boldsymbol{H} = \boldsymbol{A}_{\mathrm{Rx}}^* \boldsymbol{D} \boldsymbol{A}_{\mathrm{Tx}}^{\mathrm{T}} \in \mathbb{C}^{M_r \times M_t},$$

where $\boldsymbol{A}_{\mathrm{Rx}} \in \mathbb{C}^{M_r \times L}$ is the receive steering matrix with entries $a_{m,\ell}^{\mathrm{Rx}}$, $\boldsymbol{A}_{\mathrm{Tx}} \in \mathbb{C}^{M_t \times L}$ is the transmit steering matrix with entries $a_{n,\ell}^{\mathrm{Tx}}$ and $\boldsymbol{D} \in \mathbb{C}^{L \times L}$ is a diagonal matrix with entries d_ℓ on its main diagonal.

For a given set of parameters $\{\alpha_\ell, \tau_\ell, \vec{\Omega}_\ell^{\mathrm{Tx}}, \vec{\Omega}_\ell^{\mathrm{Rx}}, L\}$, which characterizes a particular propagation environment with an associated stationarity region E, short-term fading can be simulated by inserting a trajectory $\vec{r}^{\,\mathrm{Rx}}(t)$ for the mobile unit and a rotation $\vec{r}_m^{\,\mathrm{Rx}}(t)$ for its array elements in Eq. 1. On the other hand, a stochastic characterization of $\vec{r}^{\,\mathrm{Rx}}$ and $\vec{r}_m^{\,\mathrm{Rx}}$ leads to a stochastic characterization of the short-term fading of the MIMO channel. Note that since arrays are normally rigid structures, the position of an array element with respect to $\mathcal{O}_{\mathrm{Rx}}$ completely determines the position of the other array elements.

Considering a stochastic characterization of the MIMO channel, if we assume the phases of d_ℓs as i.i.d. according to a uniform distribution between 0 and 2π[1], the transmit correlation matrix is given by,

$$\boldsymbol{R}_{\mathrm{Tx}} = \mathrm{E}\{\boldsymbol{H}^{\mathrm{H}}\boldsymbol{H}\} = M_r \boldsymbol{A}_{\mathrm{Tx}}^* \boldsymbol{D}^{\mathrm{H}} \boldsymbol{D} \boldsymbol{A}_{\mathrm{Tx}}^{\mathrm{T}}. \quad (2)$$

This matrix constitutes all knowledge available at the transmitter in the partial CSI approach.

The channel model presented in this section is highly flexible in that it can model all the essential transformations that a signal suffers in its way from transmitter to receiver and the variations of those in space, frequency and time. Moreover, rather than making assumptions regarding statistical distibutions and correlations, the model relies on the choice of a set of basic parameters which render the relationship of it to the physical propagation environment completely visible.

III. Simulation Settings

Three different channels have been considered for simulation. Azimuth-delay diagrams for these three channels are depicted in Figs. 2, 3 and 4. There, directions of departure are represented with solid lines terminated by circles and directions of arrival with dotted lines terminated by triangles. The radial axis represents time in sampling intervals.

Channel A consists of two temporal taps and exhibits high spatial correlation at the transmitter, i.e. directions of departure $\vec{\Omega}_\ell^{\mathrm{Tx}}$ form a narrow circular sector. This channel could match a rural environment with few scatterers around the transmit array. Channel B consists of a cluster of 24 exponentially decaying taps and shows moderate spatial correlation at the transmitter. An urban scenario with many scatterers on and around the line of sight could be well described by channel B. Finally, channel C consists of two clusters with 8 exponentially decaying taps each; angles of departure are largely dispersed between 0° and 180°. Here, two clusters of reflectors dominate propagation of the first arriving waves and a group of far reflectors, e.g. high-rise buildings, brings about a third cluster of delayed waves (cf. [11]).

The system considered in our work operates at 5 Ghz. Uniform linear arrays (ULA) with 4 elements and a spacing of $\lambda/2$ are considered at both transmitter and receiver. These are assumed to lie on the horizontal line of the depicted azimuth-delay diagrams. The number of subcarriers is 1024 and the duration of an OFDM symbol (without cyclic prefix) is 7.58 μs. The duration of a frame amounts to 0.592 ms, which corresponds to 64 OFDM symbols with cyclic prefix.

For simulation purposes the channel is assumed stationary, i.e. the mobile unit does not leave the stationarity region. At the beginning of a frame a new starting point $\vec{r}^{\,\mathrm{Rx}}(t=0)$ is randomly chosen and movement is simulated by plugging $\vec{r}^{\,\mathrm{Rx}}(t) = \vec{r}^{\,\mathrm{Rx}}(t=0) + \vec{v}t$ into Eq. 1. Rotations of the receive array are not considered. The angle of $\vec{v}$ is drawn at the

[1]If we assume a circular E, the distribution of phases between 0 and 2π is uniform for radii of E as small as some few wavelengths (5λ). As for independence, a radius of hundreds of wavelengths guarantees independence even for a difference in the direction of arrival as small as 1 .

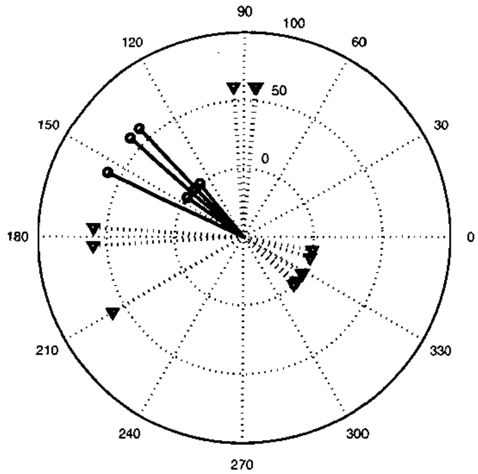

Fig. 2. Channel A

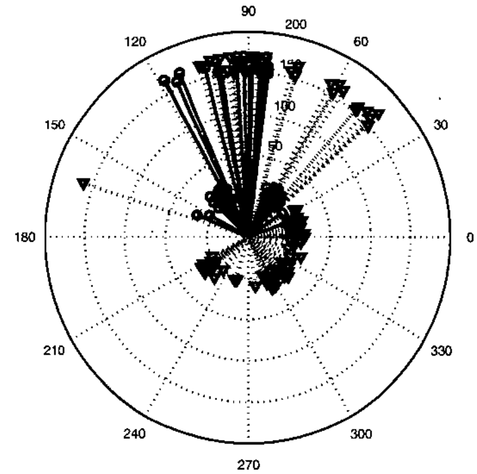

Fig. 4. Channel C

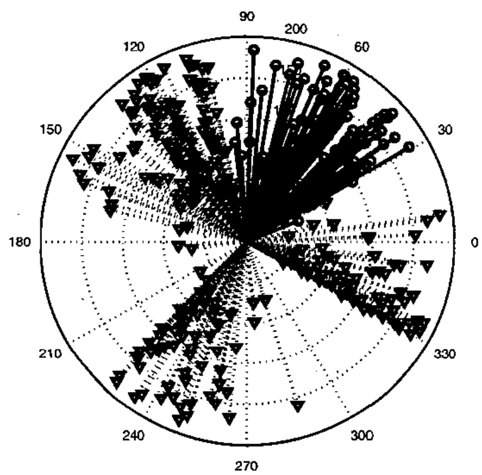

Fig. 3. Channel B

beginning of each frame according to a uniform distribution between 0 and 2π. Performance is evaluated at speeds 10 Km/h, 60 Km/h and 300 Km/h. Transmission is uncoded with an spectral efficiency of 4 bits/subcarrier.

For each subcarrier k, the transmission model reads,

$$\boldsymbol{y}_k(t) = \boldsymbol{H}(f_k,t)\boldsymbol{U}_k(t)\boldsymbol{P}_k(t)^{1/2}\boldsymbol{x}_k(t) + \boldsymbol{n}_k(t),$$

where $\boldsymbol{y}_k(t)$ and $\boldsymbol{x}_k(t)$ are vectors of receive and transmit signals, respectively, at time t, $\boldsymbol{n}_k(t)$ is a white Gaussian noise vector, $\boldsymbol{P}_k(t)$ is a diagonal matrix assigning power to the space-frequency signal components, $\boldsymbol{U}_k(t)$ is a unitary precoding matrix and $\boldsymbol{H}(f_k,t)$ is the transfer function of the channel at subcarrier frequency f_k. This model assumes the absence of intersymbol and intercarrier interference, which applies for the system and channels considered here.

For perfect CSI, precoding matrices are applied which achieve channel diagonalization. Such precoding has been shown to preserve capacity in [2]. Subsequently, for each OFDM symbol bit and power loading is performed over the resulting space-frequency components based on the algorithm presented in [12]. In this case the V-BLAST detector reduces to a unitary transformation that diagonalizes the channel and an inversion of the resulting subchannels as long as CSI at the transmitter does not become obsolete, i.e. V-BLAST is equivalent to a maximum likelihood (ML) receiver. For the case of obsolete perfect CSI precoding matrices and bit and power loading are only computed for the first OFDM symbol and used unchanged for the rest of the frame.

For the case of no CSI, simple spatial multiplexing is applied at the transmitter with a uniform distribution of bits and power along frequency and antennas. Precoding matrices are unity matrices.

Finally, for the case of partial CSI the adaptive procedure described in a companion paper [13] is used to perform bit and power loading over eigenbeams, which result if the matrix of eigenvectors of the transmit correlation matrix is applied as precoding matrix. This precoding has been shown to be optimum for Rayleigh-fading MIMO channels in [14]. Since the channel is stationary, precoding and loading do not change over time. Furthermore, it can be verified that variation with frequency of eigenvectors and eigevalues is negligible for a system as the one considered here. This means that only the estimation of a correlation matrix is required to perform signal processing at the transmitter over the whole spectrum, which is an important complexity reduction with respect to the case of perfect CSI, where at least the estimation of $N+1$ matrices is required, N being the order of the channel.

IV. Simulation Results

In Figs. 5, 6, 7 performance curves are plotted for the three channels introduced in Section III. For channel A, the performance gap between partial CSI and perfect CSI is relatively small. Due to the strong spatial correlation, the covariance matrix has only one dominant eigenvalue, which characterizes the spatial structure of any channel realization. Only knowledge about the spectral characteristic of the channel, which partial CSI does not provide, makes the difference. Degradation increases with growing speed as it could be expected. In the low SNR region, performance is limited by noise and CSI obsolescence brings about a negligible performance loss. In the high SNR region, performance is more sensitive to CSI and hence degradation increases. Due to mobility the match between the power and bit loadings computed at the beginning of the frame and the spectral characteristic of the actual channel realization gradually vanishes, which leads to performance degradation. At 300 Km/h degradation results in BERs significantly higher than those obtained when using partial CSI.

Channels B and C behave similarly. Now, since partial CSI provides less information about the spatial structure of the actual channel realization, the performance gap with respect to perfect CSI increases. Furthermore, precoding computed with perfect CSI at the beginning of the frame becomes now obsolete as time elapses. Note that in channel A, due to high spatial correlation, precoding does not substantially change over different channel realizations. This leads to a more severe performance degradation in channels B and C compared to channel A. However, even at a speed of 300 Km/h degradation is compensated with high transmission reliability at the beginning of the frame, which results in an average performance similar to that obtained by using partial CSI.

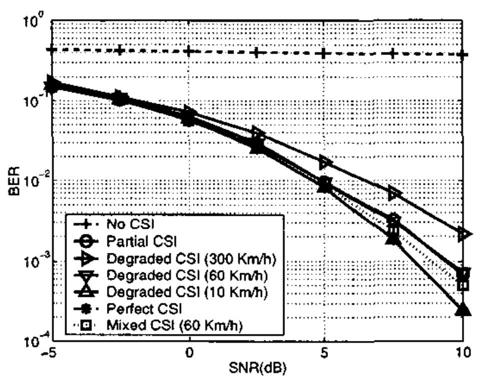

Fig. 5. Performance curves (channel A)

Fig. 8 shows performance degradation over time for channel C at SNR = 5 dB. Also plotted is the BER obtained with partial CSI, which, of course, does not change either with time or velocity. We observe that at 10 Km/h degradation is completely negligible. At 60 Km/h degradation occurs but still BER is significantly lower than that obtained with partial CSI. Finally, at 300 Km/h there is a crossover of the curves corresponding to partial and degraded CSI after 200 ms. Loss of correlation between channel realizations at the beginning of

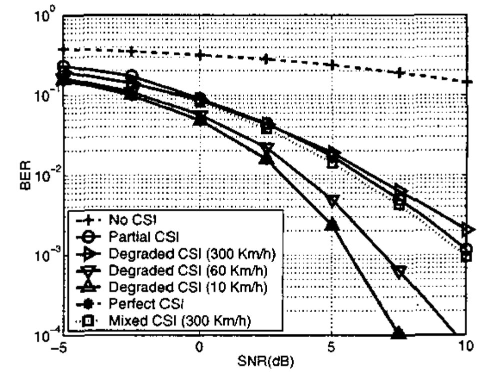

Fig. 6. Performance curves (channel B)

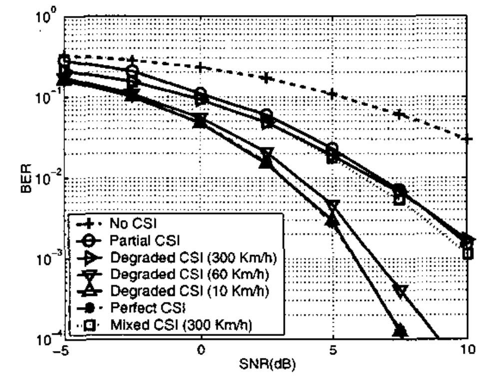

Fig. 7. Performance curves (channel C)

the frame and those resulting from change of location during the transmission of the frame is responsible for performance degradation over time. Coming back to our channel model and making the same assumptions that led to Eq. 2, it is easy to show that, considering an angle of $\vec{v}$, viz. θ_v, uniformly distributed between 0 and 2π, the following autocorrelation function results for the stationary channel,

$$\boldsymbol{R}_{\mathrm{Tx}}(t) =$$

$$\mathrm{E}_{\vec{r}_{\mathrm{Rx}},\theta_v}\{\boldsymbol{H}^{\mathrm{H}}(\vec{r}_{\mathrm{Rx}}+\vec{v}t)\boldsymbol{H}(\vec{r}_{\mathrm{Rx}})\} = J_0\left(\frac{2\pi}{\lambda}|\vec{v}|t\right)\boldsymbol{R}_{\mathrm{Tx}},$$

where $J_0(x)$ is the Bessel function of the first kind and order 0. Fig. 9 shows $J_0(2\pi|\vec{v}|t/\lambda)$ for the three speeds considered here. Observing both Figs. 8 and 9, dependence of performance degradation with correlation between obsolete and actual channel realizations becomes clear.

Finally, we have investigated the ideal case in which the base station knows the crossover point between the BER curves corresponding to partial and degraded CSI and preprocesses the OFDM symbols according to the most favorable approach at a given instant of time, i.e. at the beginning of the frame degraded CSI is used and after the crossover point

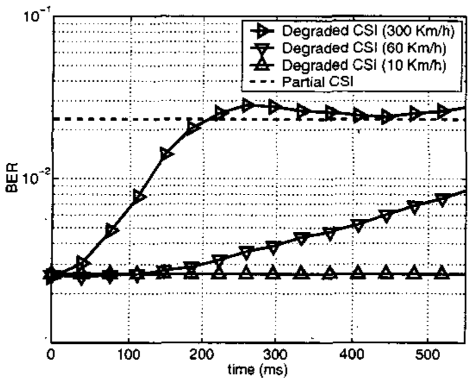

Fig. 8. Performance degradation at SNR = 5dB (Channel C)

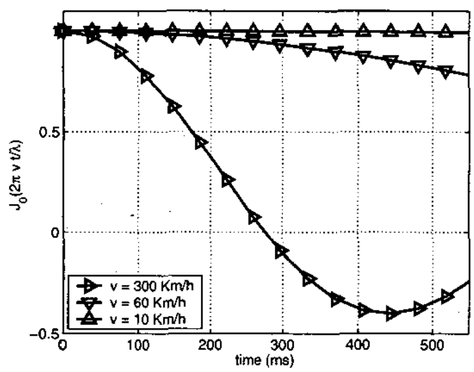

Fig. 9. Autocorrelation function

processing based on partial CSI is performed. The resulting BER curves over SNR are depicted in Figs. 5, 6, 7 and referred to as "mixed CSI". The gain obtained from such an ideal switching method turns out to be rather modest. Better perfomance can be expected from a method that, instead of hardly switching, considers both degraded and partial CSI for preprocessing purposes from the very beginning of the frame. This kind of CSI-adaptive processing design constitutes an interesting topic for further research.

V. Conclusions

A chanel model has been introduced that allows both a deterministic and stochastic characterization of the MIMO channel. Using this model, downlink performance of a TDD MIMO/OFDM system has been investigated for three particular channels and different degrees of CSI at the transmitter.

For correlated channels, e.g. channel A, partial CSI offers the best trade-off between performance and complexity at all speeds. For moderately and weakly correlated channels, e.g. channels B and C, partial CSI still provides a large performance gain with respect to the case with no CSI at the transmitter but is largely outperformed by perfect CSI with obsolescence at low and moderate speeds. Only at very high speeds is performance of partial and degraded CSI similar. In this kind of scenarios the estimation of the channel could be worth the associated computational cost.

Finally, it should be mentioned that the same evaluation with coded transmission would narrow the performance gap between curves since lack of knowledge can then be partially compensated by diversity. In that case conclusions could be slightly different.

VI. Acknowledgement

The authors would like to thank DoCoMo Eurolabs for the support of this work.

References

[1] B. of Visions, *Visions of a Wireless World.* WWRF, 2001.

[2] G. G. Raleigh and J. M. Cioffi, "Spatio-Temporal Coding for Wireless Communication," *IEEE Trans. Communications*, vol. 46, pp. 357–366, 1998.

[3] K. K. Wong, R. K. Lai, R. S. K. Cheng, K. B. Letaief, and R. D. Murch, "Adaptive Spatial-Subcarrier Trellis Coded MQAM and Power Optimization for OFDM Transmission," in *IEEE Vehicular Technology Conference (VTC)*, Tokyo, Japan, May 2000.

[4] P. Bansal and A. Brzezinski, "Adaptive Loading in MIMO/OFDM System," Available at www.stanford.edu/ brzezin/359/359.pdf, 2001.

[5] G. G. Raleigh and V. K. Jones, "Multivariate Modulation and Coding for Wireless Communication," *IEEE Journal on Selected Areas in Communications*, vol. 17, pp. 357–366, May 1999.

[6] D. Agrawal, V. Tarokh, A. Naguib, and N. Seshadri, "Space-Time Coded OFDM for High Data-Rate Wireless Communication Over Wideband Channels," in *IEEE Vehicular Technology Conference (VTC)*, May 1998.

[7] Z. Liu, Y. Xin, and G. B. Giannakis, "Space-Time-Frequency Coded OFDM Over Frequency-Selective Fading Channels," *IEEE Trans. Signal Processing*, vol. 50, pp. 2465–2476, Oct. 2002.

[8] H. W. Wolniansky, G. J. Foschini, and R. A. Valenzuela, "V-BLAST: An Architecture for Realizing Very High Data Rates Over the Rich-Scattering Wireless Channel," in *URSI International Symposium on Signals, Systems, and Electronics*, New York, 1998, pp. 295–300.

[9] H. Bölcskei, D. Gesbert, and A. J. Paulraj, "On the Capacity of OFDM-Based Spatial Multiplexing Systems," vol. 50, pp. 225–234, 2002.

[10] E. Bonek, H. Hofstetter, C. F. Mecklenbräuker, and M. Steinbauer, "Double-directional Superresolution Radio Channel Measurements," in *39th Annual Allerton Conference on Communication, Control and Computing*, Monticello, IL, USA, Oct. 2001.

[11] M. Toeltsch, J. Laurila, K. Kalliola, A. F. Molisch, P. Vainikainen, and E. Bonek, "Statistical Characterisation of Urban Spatial Radio Channels," vol. 20, pp. 1–27, April, 2002.

[12] R. F. H. Fischer and J. B. Huber, "A New Loading Algorithm for Discrete Multitone Transmission," in *Globecom*, 1996, pp. 724–728.

[13] P. Tejera, W. Utschick, G. Bauch, and J. A. Nossek, "Joint Bit and Power Loading for MIMO OFDM based on Partial Channel Knowledge," in *IEEE Vehicular Technology Conference (VTC)*, Milan, Italy, May 2004.

[14] S. A. Jafar, S. Vishwanath, and A. Goldsmith, "Channel Capacity and Beamforming for Multiple Transmit and Receive Antennas with Covariance Feedback," in *International Conference on Communications*, 2001.